A consecutive modal pushover procedure for nonlinear static analysis of one-way unsymmetric-plan tall building structures

Mehdi Poursha [a,*], Faramarz Khoshnoudian [b], A.S. Moghadam [c]

[a] Department of Civil Engineering, Sahand University of Technology, Tabriz, Iran
[b] Department of Civil Engineering, Amirkabir University of Technology, Tehran, Iran
[c] International Earthquake and Seismology Research Centre, Tehran, Iran

ARTICLE INFO

ABSTRACT

Seismic responses of unsymmetric-plan tall buildings are substantially influenced by the effects of higher modes and torsion. Considering these effects, in this article, the consecutive modal pushover (CMP) procedure is extended to estimate the seismic demands of one-way unsymmetric-plan tall buildings. The procedure uses multi-stage and classical single-stage pushover analyses and benefits from the elastic modal properties of the structure. Both lateral forces and torsional moments obtained from modal analysis are used in the multi-stage pushover analysis. The seismic demands are obtained by enveloping the peak inelastic responses resulting from the multi-stage and single-stage pushover analyses. To verify and appraise the procedure, it is applied to the 10, 15, and 20-storey one-way unsymmetric-plan buildings including systems with different degrees of coupling between the lateral displacements and torsional rotations, i.e. torsionally-stiff (TS), torsionally-similarly-stiff (TSS) and torsionally-flexible (TF) systems. The modal pushover analysis (MPA) procedure is implemented for the purpose of comparison as well. The results from the approximate pushover procedures are compared with the results obtained by the nonlinear response history analysis (NL-RHA). It is demonstrated that the CMP procedure is able to take into account the higher mode influences as well as amplification or de-amplification of seismic displacements at the flexible and stiff edges of unsymmetric-plan tall buildings. The extended procedure can predict to a reasonable accuracy the peak inelastic responses, such as displacements and storey drifts. The CMP procedure represents an important improvement in estimating the plastic rotations of hinges at both flexible and stiff sides of unsymmetric-plan tall buildings in comparison with the MPA procedure.

© 2011 Elsevier Ltd. All rights reserved.

1. Introduction

The nonlinear static procedure or pushover analysis is increasingly used to establish the estimations of seismic demands for building structures. The pushover analysis is, however, restricted with a single-mode response. Then, the use of this procedure for unsymmetric-plan or tall buildings yields erroneous results. In order to cope with this limitation, attempts have been made to develop enhanced pushover procedures. During past years, multi-mode pushover (MMP) method [1], modal pushover analysis (MPA) [2], pushover results combination (PRC) [3], incremental response spectrum analysis (IRSA) [4], upper-bound pushover analysis [5], modified modal pushover analysis (MMPA) [6], adaptive modal combination (AMC) procedure [7] and improved modal pushover analysis [8] were proposed to consider the effects of

higher modes. Lately, the consecutive modal pushover (CMP) procedure [9] was also developed in which the structural responses were obtained by enveloping the results of multi-stage and conventional single-stage pushover analyses. The CMP procedure was shown to be effective in predicting the seismic demands of tall buildings.

The above-mentioned procedures were limited to planar frames and symmetric buildings. Several research efforts have been made to extend and apply the pushover analysis to unsymmetric-plan buildings whose inelastic seismic responses are intricate. Kilar and Fajfar [10,11], De Stefano and Rutenberg [12], Faella and Kilar [13], Moghadam and Tso [14,15], Ayala et al. [16], Fujii et al. [17] and Barros and Almeida [18] investigated on the application of pushover analysis for seismic evaluation of unsymmetric-plan buildings. Recently, the modal pushover analysis (MPA) [19], the N2 method [20,21] and a simplified seismic analysis [22] were extended to the unsymmetric-plan buildings. In the MPA procedure, torsional moments were applied in addition to lateral forces at each floor level. The seismic demands were separately calculated for each of the modal pushover analyses and combined by

---

using the CQC modal combination scheme. The MPA procedure is unable to accurately predict the plastic rotation of hinges. In the extended N2 method, the results produced by pushover analysis (based on the N2 method) were combined with the results from elastic spectral analysis by using a correction factor. The former results control the target displacements and distribution of deformations along the height of the building, while the latter results are used to account for the torsional amplifications. The correction factor was defined as the ratio between the normalized roof displacements derived from elastic spectral analysis and those resulting from pushover analysis. De-amplification of displacements due to torsion was not taken into consideration in the method. This method is limited to low-rise buildings where the higher mode effects are not significant. Also, nonlinear static analysis methods including the N2 and MPA methods were assessed for unsymmetric-plan low-rise buildings [23]. Until recently, little attention has been paid to unsymmetric-plan tall buildings to develop a pushover analysis procedure which can provide satisfactory estimates of the hinge plastic rotations.

The main objective of this paper is to extend the consecutive modal pushover (CMP) procedure to the one-way unsymmetric-plan tall buildings in which torsional and higher mode effects play an important role in estimating the seismic responses. An outline of this paper can be expressed as follows. First, necessary modal properties of multi-storey buildings with one-way unsymmetric-plan are demonstrated. Then, three types of unsymmetric-plan buildings from the perspective of degrees of coupling between the translational displacements and torsional rotations are described. Next, the fundamental bases and details of the CMP procedure extended to the unsymmetric-plan tall buildings are presented. Subsequently, a brief description of structural models, underlying assumptions and used ground motions are given. At the end, predictions resulting from the CMP procedure are shown and compared with the results of benchmark solution, i.e. nonlinear response history analysis (NL-RHA). In addition, a comparison of the estimates from the proposed procedure to those from the MPA procedure is conducted. Results evaluation and relevant discussion are presented in detail. Particular emphasis is placed on the considerable progress through the CMP procedure in predicting the plastic hinge rotations of unsymmetric-plan tall buildings for the frames at the flexible and stiff sides.

2. Modal properties of multi-storey buildings with one-way unsymmetric-plan

The differential equations governing the response of multi-storey buildings with arbitrary plan to the horizontal components of ground motion, i.e. $\ddot{u}_{gx}(t)$ and $\ddot{u}_{gy}(t)$ in the x- and y- directions, respectively, are as follows [24,19]:

$$\mathbf{M}\ddot{\mathbf{u}} + \mathbf{f_s} = -\mathbf{M}\mathbf{i}_x\ddot{u}_{gx}(t) - \mathbf{M}\mathbf{i}_y\ddot{u}_{gy}(t) \quad (1)$$

in which $\mathbf{M}$ is a diagonal mass matrix of order $3N$. The matrix, $\mathbf{M}$, includes three diagonal sub-matrices $\mathbf{m}$, $\mathbf{m}$ and $\mathbf{I_o}$, each of order N; $\mathbf{m}$ is a diagonal matrix with $m_{jj} = m_j$, the mass lumped at the jth floor diaphragm. $\mathbf{I_o}$ is a diagonal matrix with $I_{jj} = I_{oj}$, the polar moment of inertia of the jth floor diaphragm about a vertical axis through the centre of mass (CM). The influence vectors, $\mathbf{i}_x$ and $\mathbf{i}_y$, which are associated with the components of ground motion in the x- and y-directions, respectively, are as follows:

$$\mathbf{i}_x = \begin{Bmatrix} \mathbf{1} \\ \mathbf{0} \\ \mathbf{0} \end{Bmatrix} \qquad \mathbf{i}_y = \begin{Bmatrix} \mathbf{0} \\ \mathbf{1} \\ \mathbf{0} \end{Bmatrix} \quad (2)$$

where each element of the $N \times 1$ vector $\mathbf{1}$ is equal to unity and of the $N \times 1$ vector $\mathbf{0}$ is equal to zero. The displacement vector, $\mathbf{u}$, of size $3N \times 1$ includes three $N \times 1$ sub-vectors $\mathbf{u}_x$, $\mathbf{u}_y$,
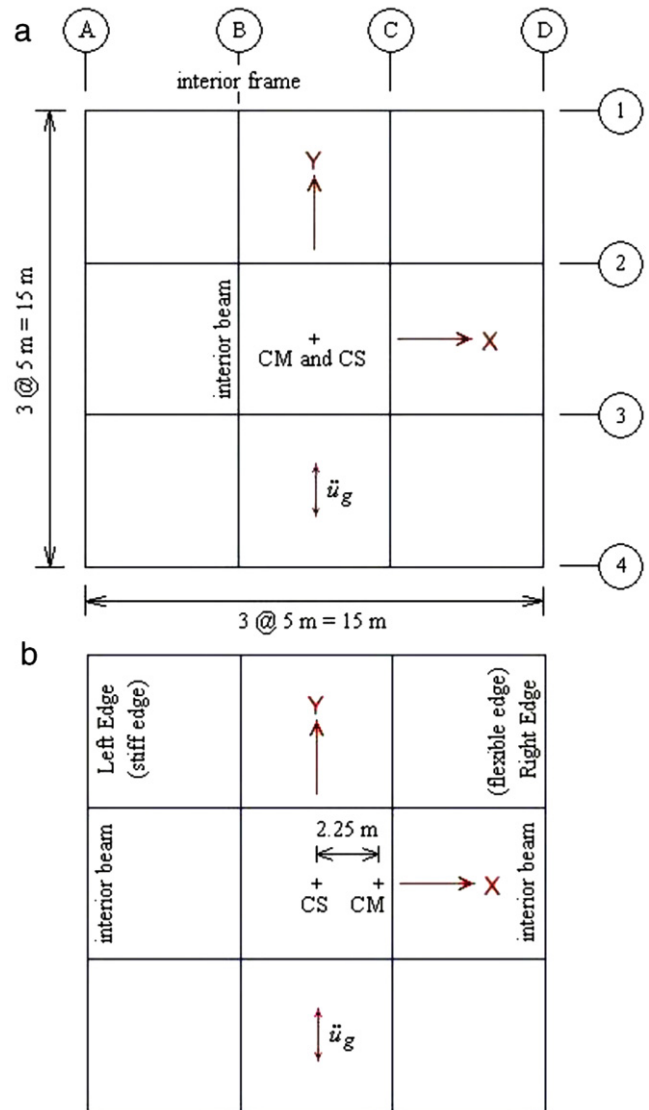

Fig. 1. Plan of the analysed tall buildings: (a) the original symmetric-plan buildings; (b) the created one-way unsymmetric-plan buildings.

and $\mathbf{u}_\theta$ whose elements denote the x- and y-lateral and torsional floor displacements, respectively. Eq. (1) is specialized for one-way unsymmetric-plan buildings, i.e. symmetric about x-axis but unsymmetric about y-axis [see Fig. 1(b)], subjected to earthquake ground motion in the y-direction. It can then be expressed as

$$\begin{bmatrix} \mathbf{m} & \mathbf{0} \\ \mathbf{0} & \mathbf{I_o} \end{bmatrix} \begin{Bmatrix} \ddot{u}_y \\ \ddot{u}_\theta \end{Bmatrix} + \begin{bmatrix} \mathbf{k}_{yy} & \mathbf{k}_{y\theta} \\ \mathbf{k}_{\theta y} & \mathbf{k}_{\theta\theta} \end{bmatrix} \begin{Bmatrix} u_y \\ u_\theta \end{Bmatrix} = -\begin{bmatrix} \mathbf{m} & \mathbf{0} \\ \mathbf{0} & \mathbf{I_o} \end{bmatrix} \begin{Bmatrix} \mathbf{1} \\ \mathbf{0} \end{Bmatrix} \ddot{u}_{gy}(t) \quad (3)$$

in which $\mathbf{k}_{yy}$, $\mathbf{k}_{y\theta}$, $\mathbf{k}_{\theta y}$ and $\mathbf{k}_{\theta\theta}$ are the stiffness sub-matrices. When all floor diaphragms have the same radius of gyration ($I_{oj} = m_j r^2$), the sub-matrix, $\mathbf{I_o}$, can be substituted with $\mathbf{I_o} = r^2\mathbf{m}$ in the above equation.

The effective earthquake forces, $\mathbf{P_{eff}}(t)$, are defined by the right side of Eq. (3):

$$\mathbf{P_{eff}}(t) = -\begin{Bmatrix} \mathbf{m1} \\ \mathbf{0} \end{Bmatrix} \ddot{u}_{gy}(t) = -\mathbf{s}\ddot{u}_{gy}(t). \quad (4)$$

The spatial distribution, $\mathbf{s}$, of the effective earthquake forces can be expanded as a summation of modal inertia force distributions,

s_n, as follows:

$$\mathbf{s} = \begin{Bmatrix} \mathbf{m1} \\ \mathbf{0} \end{Bmatrix} = \sum_{n=1}^{2N} \mathbf{s}_n = \sum_{n=1}^{2N} \Gamma_n \begin{Bmatrix} \mathbf{m}\Phi_{yn} \\ r^2\mathbf{m}\Phi_{\theta n} \end{Bmatrix} \tag{5}$$

in which Φ_{yn} and $\Phi_{\theta n}$ include the translations and rotations of the N floors about a vertical axis for the nth mode $\left(\Phi_n = \left\{\Phi_{yn}^T \quad \Phi_{\theta n}^T\right\}\right)$, respectively. Modal participating factor, Γ_n, is defined as follows:

$$\Gamma_n = \frac{L_n}{M_n} \tag{6}$$

where

$$L_n = \left\{\Phi_{yn}^T \quad \Phi_{\theta n}^T\right\} \begin{Bmatrix} \mathbf{m1} \\ \mathbf{0} \end{Bmatrix} = \Phi_{yn}^T \mathbf{m1} = \sum_{j=1}^{N} m_j \phi_{jyn} \tag{7}$$

$$M_n = \left\{\Phi_{yn}^T \quad \Phi_{\theta n}^T\right\} \begin{bmatrix} \mathbf{m} & \mathbf{0} \\ \mathbf{0} & r^2\mathbf{m} \end{bmatrix} \begin{Bmatrix} \Phi_{yn} \\ \Phi_{\theta n} \end{Bmatrix} \tag{8}$$

where M_n can be expanded as follows:

$$M_n = \Phi_{yn}^T \mathbf{m}\Phi_{yn} + r^2\Phi_{\theta n}^T \mathbf{m}\Phi_{\theta n}$$

$$= \sum_{j=1}^{N} m_j \phi_{jyn}^2 + r^2 \sum_{j=1}^{N} m_j \phi_{j\theta n}^2. \tag{9}$$

Two notable results are obtained by pre-multiplying each sub-matrix equation in Eq. (5) by $\mathbf{1}^T$:

$$\sum_{n=1}^{2N} M_n^* = \sum_{j=1}^{N} m_j \qquad \sum_{n=1}^{2N} I_{on}^* = 0 \tag{10}$$

in which

$$M_n^* = \frac{(L_n)^2}{M_n} \qquad I_{on}^* = r^2 \Gamma_n \mathbf{1}^T \mathbf{m}\Phi_{\theta n} \tag{11}$$

where M_n^* and I_{on}^* are the effective modal mass and modal static response for base torque, respectively. Eq. (10)a shows that the sum of the effective modal masses, M_n^*, over all modes ($2N$) is equal to the total mass of the building. The effective modal participating mass ratio, α_n, can be defined as

$$\alpha_n = \frac{M_n^*}{\sum_{j=1}^{N} m_j}. \tag{12}$$

Eqs. (10) and (12) obviously demonstrate that the sum of the effective modal participating mass ratios over all modes is equal to unity.

3. Types of unsymmetric-plan buildings

From the perspective of degrees of coupling between lateral and torsional motions, the unsymmetric-plan buildings can be categorized into three different types [19] based on the period ratio which is defined as the ratio of translational period to torsional period [20]. The period ratio is denoted by Ω_y. Three types of unsymmetric-plan systems involve torsionally-stiff (TS), torsionally-similarly-stiff (TSS) and torsionally-flexible (TF) systems. In torsionally-stiff systems, lateral displacements dominate motion in the first mode and torsional rotations dominate motion in the second mode, whereas in torsionally-flexible systems, torsional rotations dominate motion in the first mode and lateral displacements dominate motion in the second mode. There is a weak coupling between lateral displacements and torsional rotations in torsionally-stiff and torsionally-flexible systems. In torsionally-similarly-stiff systems, which have very

close modal periods, there is a strong coupling between lateral and torsional motions. Consequently, the torsionally-stiff buildings can be recognized with period ratios larger than one and the torsionally-flexible buildings with period ratios less than one [20]. The period ratio is closer to unity for the torsionally-similarly-stiff systems than for the other two systems.

4. Consecutive modal pushover (CMP) procedure

The consecutive modal pushover (CMP) procedure was proposed to estimate the seismic demands of symmetric tall buildings [9]. Herein, this procedure is extended to the one-way unsymmetric-plan tall buildings. Multi-stage and single-stage pushover analyses are used in the procedure. In the multi-stage pushover analysis, modal pushover analyses are carried out continuously, so that when one stage (one modal pushover analysis) has been completely performed, the subsequent stage (subsequent modal pushover analysis) starts with an initial structural state (stress and deformation) which is the same as the condition at the end of the previous stage. The lateral forces are incrementally applied in the multi-stage pushover analysis, i.e. the forces, at the end of each stage, are preserved on the structure and the lateral forces, in the next stage, are added to those at the end of the previous stage. Also, the multi-stage pushover analysis is performed in such a way that the controlled point at the roof deforms in one direction during different stages of analysis. The number of stages in the multi-stage pushover analysis depends on the period (height) of structure and type of unsymmetric-plan building. The displacement increment at the roof, in each stage of the multi-stage pushover analysis, is determined as the product of a factor, β_i, and the total target displacement, δ_t, at the roof. The factor, β_i, is calculated from the initial modal properties of the structure. The displacement increment, u_{ri}, at the centre of mass (CM) at the roof in the ith stage of multi-stage pushover analysis, is determined as

$$u_{ri} = \beta_i \delta_t \tag{13}$$

in which

$$\beta_i = \alpha_i \quad \text{for the stages before the last stage} \tag{14}$$

and

$$\beta_i = 1 - \sum_{j=1}^{N_s-1} \alpha_j \quad \text{for the last stage} \tag{15}$$

where N_s is the number of stages in the multi-stage pushover analysis and α_i is the effective modal mass ratio for the ith mode, which is derived from Eq. (12). The absolute displacement, U_{ri}, at the roof's centre of mass, at the end of each stage, can be also calculated as follows:

$$U_{ri} = \gamma_i \delta_t \tag{16}$$

in which try

$$\gamma_i = \sum_{j=1}^{i} \alpha_j \quad \text{for the stages before the last stage} \tag{17}$$

and

$$\gamma_i = 1 \quad \text{for the last stage.} \tag{18}$$

It is noted that the total target displacement, at the roof, can be obtained by using conventional methods described in the guidelines, i.e., the capacity spectrum method [25], the displacement coefficient approach [26], the N2 method [27] or by using the dynamic analysis of the structure [28,29,3].

Linearly elastic modal properties are used to obtain the lateral forces ($\mathbf{s}_n^* = \mathbf{M}\Phi_n$) in the multi-stage pushover analysis. In general, the lateral forces in the multi-stage pushover analysis, which are

applied incrementally during the stages of analysis, include two lateral forces and one torque at each floor level of unsymmetric-plan buildings [19]. For the one-way unsymmetric-plan buildings (unsymmetric only in the y-direction), which are subjected to the one component of earthquake ground motion in the y-direction, the incremental lateral forces over the height of the building can be expressed as follows:

$$\mathbf{s}_n^* = \mathbf{M}\Phi_n = \begin{bmatrix} \mathbf{m} & 0 & 0 \\ 0 & \mathbf{m} & 0 \\ 0 & 0 & \mathbf{I_o} \end{bmatrix} \begin{Bmatrix} 0 \\ \Phi_{yn} \\ \Phi_{\theta n} \end{Bmatrix} = \begin{Bmatrix} 0 \\ \mathbf{m}\Phi_{yn} \\ \mathbf{I_o}\Phi_{\theta n} \end{Bmatrix}. \quad (19)$$

It is obvious from the above equation that the force distribution for each mode includes a lateral force in the y-direction and a torque at each floor level of the structure. The lateral forces in the x-direction are equal to zero.

It should be noted that the two, and three-stage pushover analyses are used in the multi-stage pushover analysis for all the systems. In the case of torsionally-similarly-stiff systems, a four-stage pushover analysis is utilized in addition to the two, and three-stage pushover analyses. A classical single-stage pushover analysis is separately performed for all the systems. At the end, the seismic responses are obtained by enveloping the peak responses derived from the multi-stage and single-stage pushover analyses since it is possible to use different pushover analyses and to envelope the results [30]. In the CMP procedure, the multi-stage pushover analyses control the responses at the mid and upper storeys of unsymmetric-plan tall buildings, whereas the responses, at the lower storeys, are controlled by the single-stage pushover analysis.

Accordingly, the CMP procedure can be expressed as a sequence of following steps:

1. Calculate the natural frequencies, ω_n, and the mode-shapes, Φ_n. The mode-shapes are normalized so that the lateral component of Φ_n, at the roof, equals unity ($\phi_{ryn} = 1$).
2. Compute the incremental lateral forces, $\mathbf{s}_n^* = \mathbf{M}\Phi_n$, over the height of the structure for different stages of multi-stage pushover analysis by using Eq. (19).
3. Compute the total target displacement, δ_t, at the roof. The target displacement increment for each stage of the multi-stage pushover analysis is obtained by Eqs. (13)–(15).
4. Apply the gravity loads and then perform the single-stage and multi-stage pushover analyses according to the following sub-steps until the control node (CM) at the roof sways to the predetermined total target displacement, δ_t.
   4.1. Perform the single-stage pushover analysis by using an inverted triangular load pattern for medium-rise unsymmetric-plan buildings and a uniform force distribution for high-rise ones until the total target displacement, δ_t, at the roof is reached. For torsionally-flexible buildings, this analysis is carried out by using the force distribution [Eq. (19)] derived from the modal properties of the fundamental effective mode which is explained later in this section.
   4.2. Perform the two-stage pushover analysis. In the First stage, implement the pushover analysis, using the force distribution $\mathbf{s}_1^* = \mathbf{M}\Phi_1$ (Eq. (19); $n = 1$), until the displacement increment at the roof reaches $u_{r1} = \beta_1\delta_t$ (Eq. (13); $i = 1$) in which $\beta_1 = \alpha_1$ (Eq. (14); $i = 1$). Subsequently, in the second stage, continue the analysis with the incremental lateral forces $\mathbf{s}_2^* = \mathbf{M}\Phi_2$ (Eq. (19); $n = 2$) until the displacement increment at the roof equals $u_{r2} = \beta_2\delta_t$ (Eq. (13); $i = 2$) where $\beta_2 = 1 - \alpha_1$ (Eq. (15); $i = 2$).
   4.3. The third analysis is a three-stage pushover analysis. The first stage is exactly the same as the first stage of the two-stage pushover analysis. After the first stage, perform the second stage of analysis using the incremental lateral forces $\mathbf{s}_2^* = \mathbf{M}\Phi_2$ (Eq. (19); $n = 2$) until the displacement increment at the roof reaches $u_{r2} = \beta_2\delta_t$ (Eq. (13); $i = 2$)

where $\beta_2 = \alpha_2$ (Eq. (14); $i = 2$). Thereafter, perform the last stage of the three-stage pushover analysis using the incremental forces $\mathbf{s}_3^* = \mathbf{M}\Phi_3$ (Eq. (19); $n = 3$). The displacement increment at the roof at this stage is equal to $u_{r3} = \beta_3\delta_t$ (Eq. (13); $i = 3$) where $\beta_3 = 1 - \alpha_1 - \alpha_2$ (Eq. (15); $i = 3$). Note that the initial condition at each stage of the analysis is the same as the state at the end of the previous stage.
   4.4. Similarly to the previous multi-stage pushover analyses described above, perform a four-stage pushover analysis. This analysis is performed for torsionally-similarly-stiff systems.
5. Calculate the peak values of the seismic responses for the single- and multi-stage pushover analyses. The peak values for these analyses are denoted by r_i. Index i denotes the number of stage(s).
6. Calculate the envelope, r, of the peak responses as follows:

$$r = \text{Max}\{r_1, r_2\} \quad \text{for the TS and TF systems with } T < 2.2 \text{ s} \quad (20)$$

$$r = \text{Max}\{r_1, r_2, r_3\} \quad \text{for the TS and TF systems with } T \geq 2.2 \text{ s} \quad (21)$$

$$r = \text{Max}\{r_1, r_2, r_3, r_4\} \quad \text{for the TSS systems} \quad (22)$$

where T is the period of mode which has the largest effective modal mass ratio for the unsymmetric-plan building in the direction under consideration. This mode is called as the fundamental effective mode in this research.

As mentioned before, in addition to the two- and three-stage pushover analyses, a multi-stage pushover analysis including more (four) stages is used in the case of the torsionally-similarly-stiff systems because these systems have a smaller effective modal mass ratio for the fundamental effective mode and a larger ratio for the higher (fourth) mode in comparison with the other systems. Then, more modes have to be included in the multi-stage pushover analysis for the torsionally-similarly-stiff systems. In the case of torsionally-flexible systems, the seismic response is qualitatively different from that obtained by static loading at the mass centre [31]. In these systems, the single-stage pushover analysis is carried out by using a force distribution derived from the fundamental effective mode having the largest effective modal mass ratio. Dynamic behaviour and modal properties can be taken into consideration by using this mode in the single-stage pushover analysis, whereas an inverted triangular or uniform force distribution is not able to take dynamic structural behaviour into consideration.

5. Definition of structural models

Unsymmetric-plan models were created from symmetric-plan models. First, symmetric-plan buildings and relevant assumptions are described. Original symmetric-plan buildings considered in this investigation were 10, 15 and 20-storey buildings which cover a wide range of periods. As shown in Fig. 1(a), all buildings were 15 m by 15 m in plan and comprised three bays in each direction. All bays were 5 m. The storey heights were equal to 3.2 m for all buildings. They were assumed to be vertically-regular. The lateral load-resisting system of the buildings was a special steel moment-resisting frame (SMRF) in both directions. $P-\Delta$ (second order) effects due to gravity loads were included, but size, strength and deformation of the panel zone were neglected. The dead and live loads were equal to 650 and 200 kg/m² on the floor area. Gravity loads were distributed through the secondary floor structure along the beams in the y-direction. Seismic effects were determined according to the requirements of Iranian code of practice for the seismic resistant design of buildings [32]. The seismic masses at all floor levels of each building were assumed to be equal and to consist of the dead load plus 20% of the live load. The buildings were designed according to the
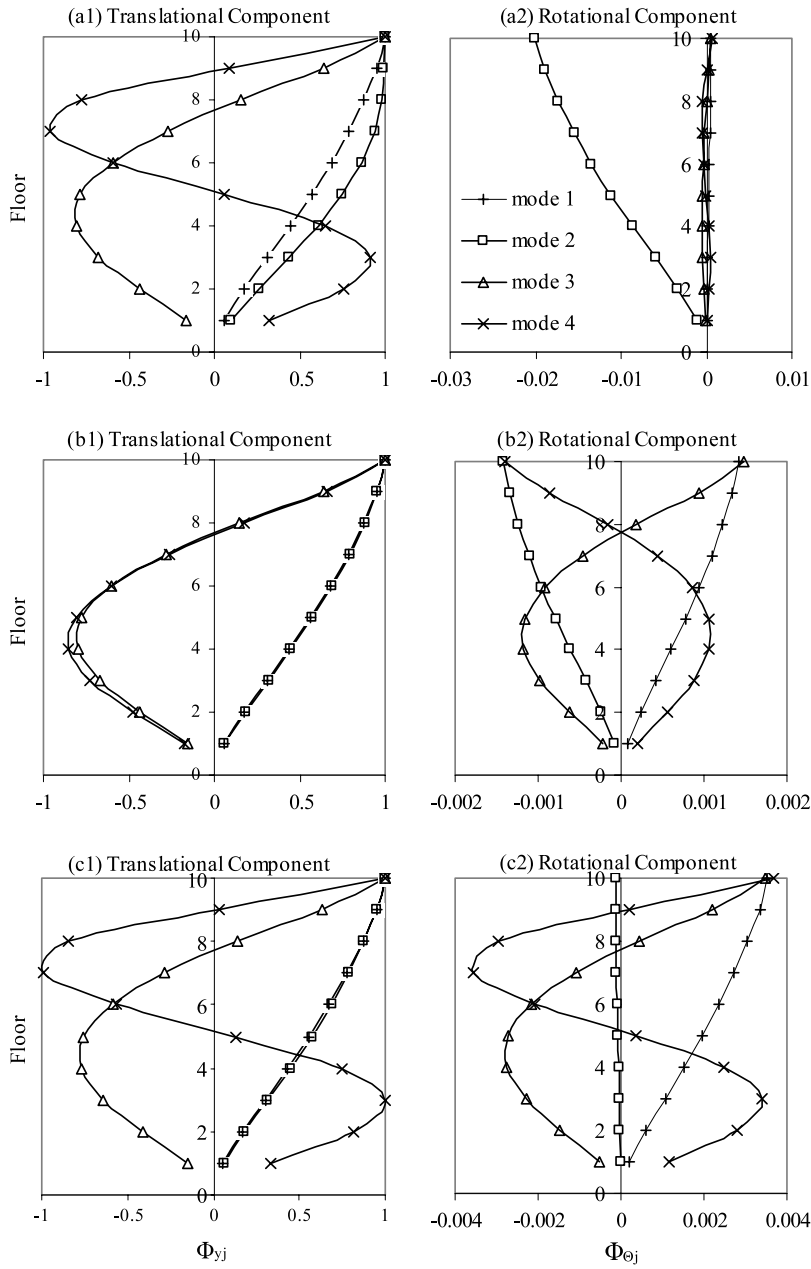
Fig. 2. Elastic mode-shapes of the 10-storey one-way unsymmetric-plan buildings: (a) torsionally-stiff system; (b) torsionally-similarly-stiff system; (c) torsionally-flexible system.
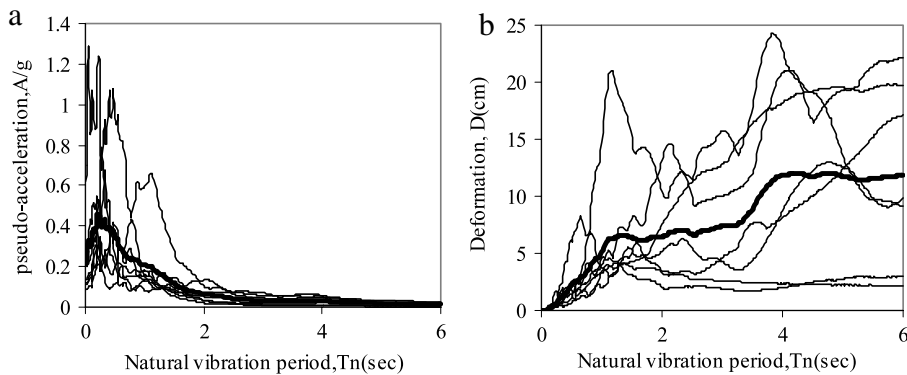

Fig. 3. (a) Pseudo-acceleration spectra and (b) displacement spectra of the set of far-field records of ground motions, damping ratio = 5%. The mean spectra are shown by a thicker line.
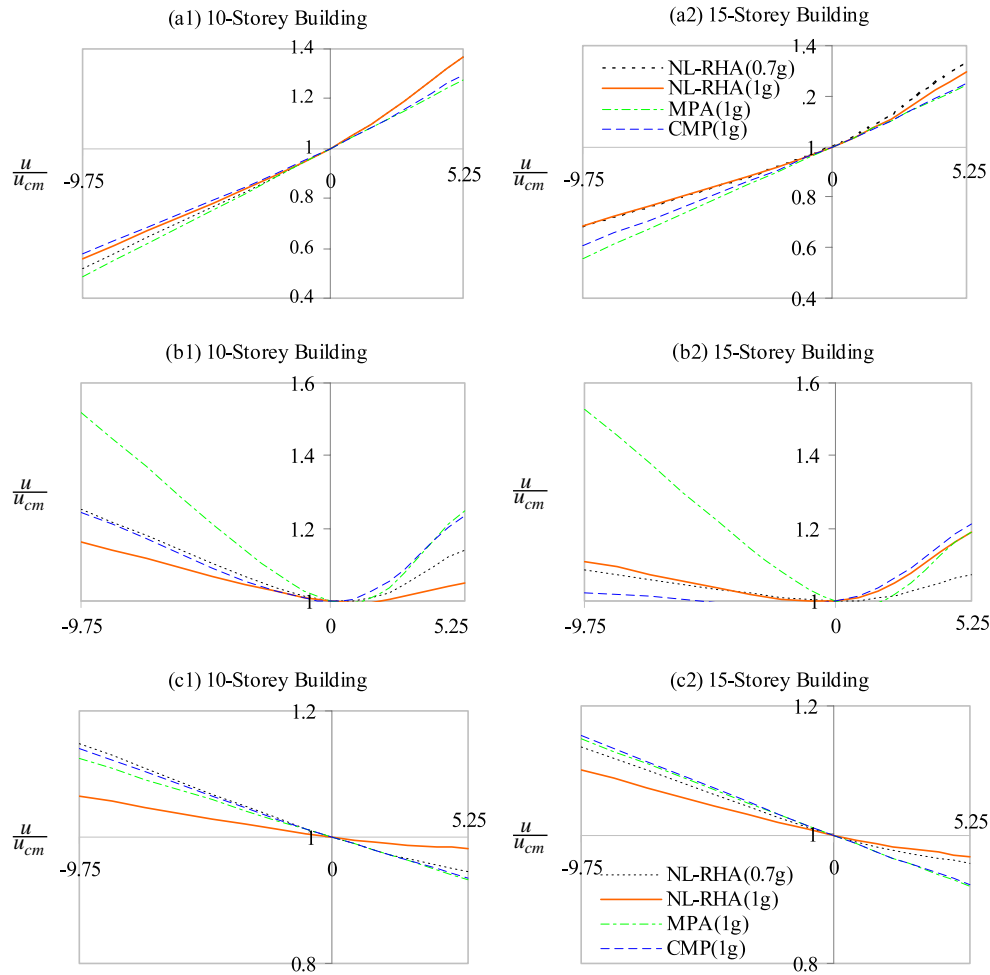
Fig. 4. Normalized displacements, $\frac{u}{u_{cm}}$, in the horizontal plane at the top floor level of the 10, and 15-storey one-way unsymmetric-plan buildings: (a) torsionally-stiff system; (b) torsionally-similarly-stiff system; and (c) torsionally-flexible system.

Table 1
Details of the analysed building structures.

Number of storeys	Total height (m)	Type of buildings	$\frac{(I_{oj}/m_j)_{unsymmetric}}{(I_{oj}/m_j)_{symmetric}}$	Periods (s)			
				T_1	T_2	T_3	T_4
10-storey	32	Symmetric	–	1.52	0.51	0.29	0.19
		TS	.28	1.63	0.69	0.55	0.31
		TSS	1.36	1.84	1.33	0.62	0.45
		TF	5.67	3.33	1.50	1.14	0.63
15-storey	48	Symmetric	–	2.33	0.82	0.48	0.40
		TS	.28	2.45	0.97	0.87	0.50
		TSS	1.59	2.76	2.05	0.98	0.72
		TF	5.67	4.66	2.29	1.65	0.97
20-storey	64	Symmetric	–	3.10	1.10	0.64	0.44
		TS	.28	3.24	1.21	1.16	0.67
		TSS	1.81	3.62	2.74	1.33	0.99
		TF	5.67	5.75	3.05	2.15	1.25

Table 2
List of the ground motions used.

| No.	Earthquake name	Date	Magnitude	Station name	Station number	Component (deg)	PGA (g)
1	Duzce, Turkey	1999/11/12	Ms (7.3)	Lamont	1,061	E	0.134
2	Northridge	1994/01/17	Ms (6.7)	LA - Baldwin Hills	24,157	90	0.239
3	Trinidad, California	1980/11/08	Ms (7.2)	Rio Dell Overpass, FF	1,498	270	0.147
4	Victoria, Mexico	1980/06/09	Ms (6.4)	Cerro Prieto	6,604	45	0.621
5	Hollister	1986/01/26	Ml (5.5)	SAGO South - Surface	47,189	295	0.09
6	Imperial Valley	1979/10/15	Ms (6.9)	Parachute Test Site	5,051	315	0.204
7	Morgan Hill	1984/04/24	Ms (6.1)	Corralitos	57,007	310	0.109
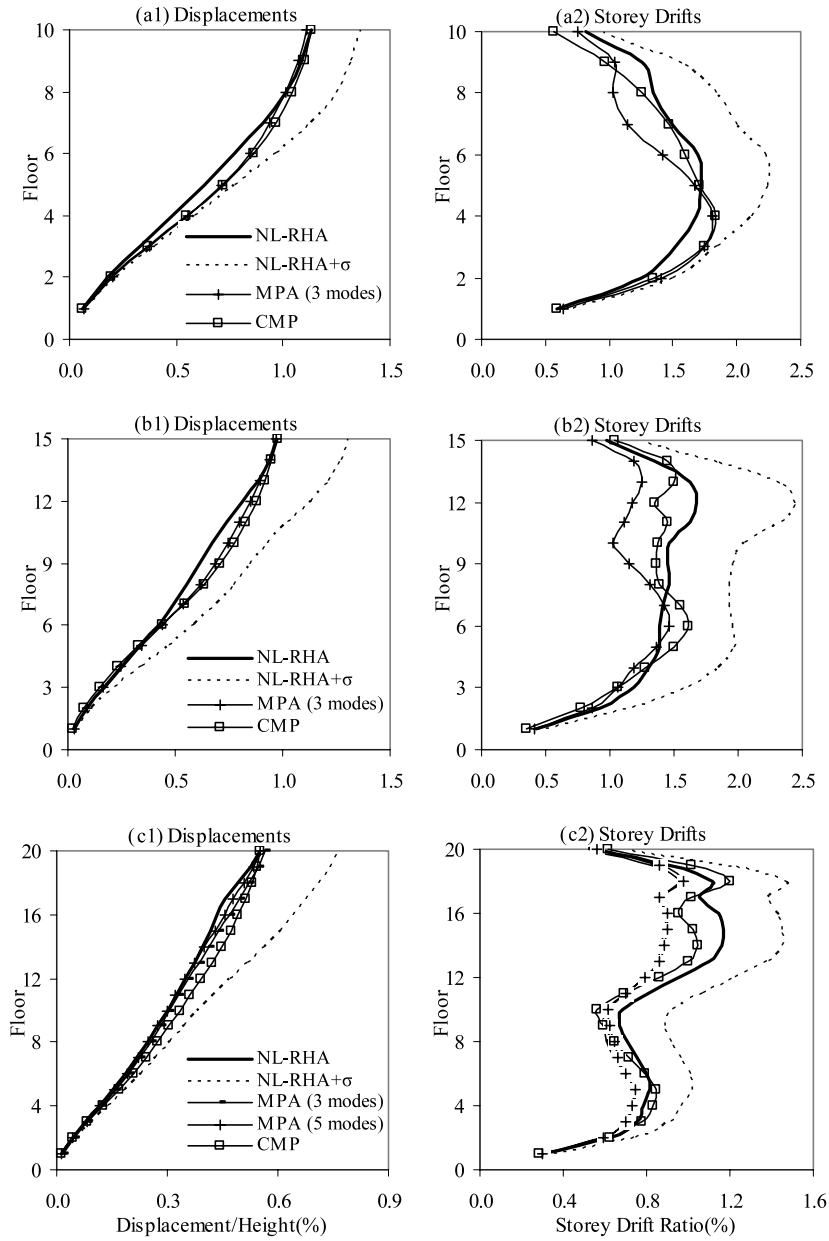
Fig. 5. Height-wise variation of the displacements and storey drifts at the CM for the original symmetric-plan buildings: (a) 10-storey building; (b) 15-storey building; and (c) 20-storey building.
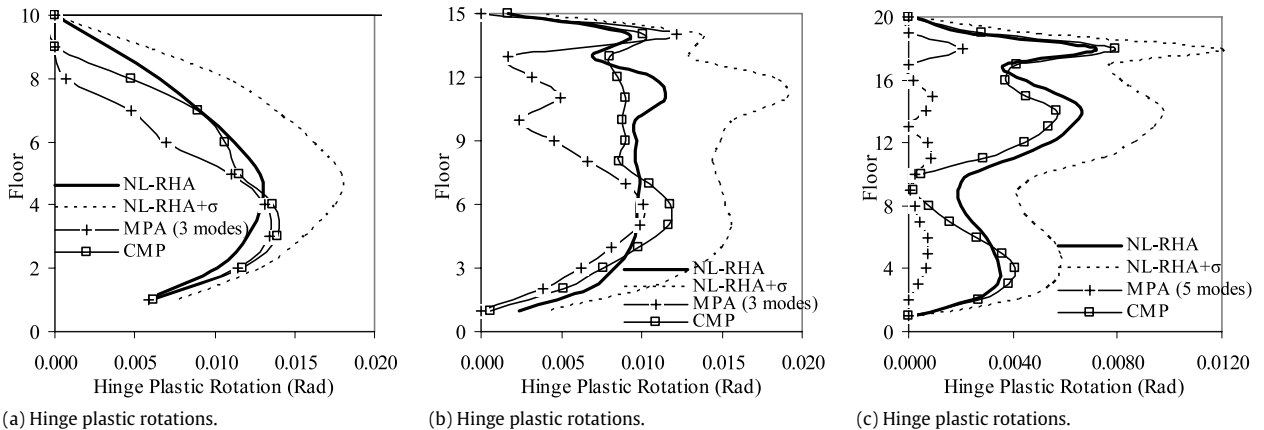

Fig. 6. Height-wise variation of the hinge plastic rotations for the original symmetric-plan buildings: (a) 10-storey building; (b) 15-storey building; and (c) 20-storey building.
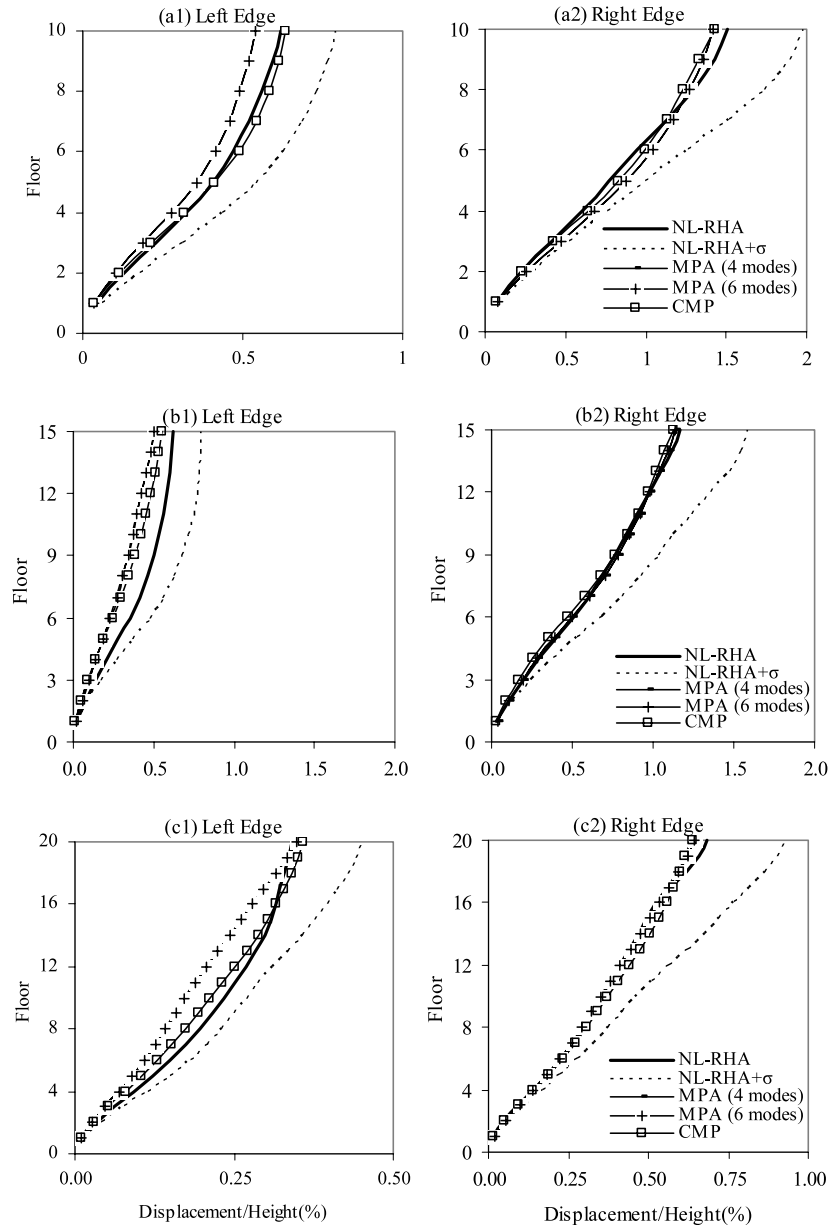
Fig. 7. Height-wise variation of the displacements at the left (stiff) and right (flexible) edges of torsionally-stiff systems: (a) 10-storey building; (b) 15-storey building; and (c) 20-storey building.

allowable stress design method [33]. The sections of the beams and columns were assumed to be of the plate girder and box type, respectively. For example, the details of the sections of the members for the 10-storey building are available in Appendix. The structures satisfied the detail requirements of the Iranian seismic code including the deformation limitation and strong column–weak beam criterion.Unsymmetric-plan buildings were considered as variations of the symmetric-plan buildings. They were assumed to be mass-eccentric and one-way unsymmetric, i.e. symmetric about x-axis but unsymmetric about y-axis. In order to create the mass-eccentric systems, symmetric-plan buildings were modified. For this purpose, the stiffness properties of each symmetric-plan building were maintained and the centre of mass (CM) was specified eccentric relative to the centre of stiffness (CS) only along the x-axis [see Fig. 1(b)]. The eccentricity between the CM and CS was assumed to be 15% of the plan dimension. Three types of unsymmetric-plan buildings were created corresponding to each of the symmetric-plan buildings by modifying the ratio of the floor moment of inertia (I_{oj}) to the floor mass (m_j) [19]. The

created systems, which have different degrees of coupling between the translational and torsional motions, involve torsionally-stiff (TS), torsionally-similarly-stiff (TSS) and torsionally-flexible (TF) systems. The ratios of the floor moment of inertia to the floor mass between the unsymmetric-plan buildings and the counterpart symmetric-plan buildings, the first four periods of linearly elastic structures, as well as the heights of all buildings are listed in Table 1. Mode-shapes of the 10-storey unsymmetric-plan buildings are shown in Fig. 2.

6. Description of analyses

To investigate the effectiveness and accuracy of the CMP procedure, which was extended to the one-way unsymmetric-plan tall buildings, the procedure together with NL-RHA were performed. The MPA procedure was also carried out for the purpose of comparison. In the MPA procedure, the seismic responses were computed for the symmetric-plan medium-rise (10- and 15-storey) buildings including three modes, for
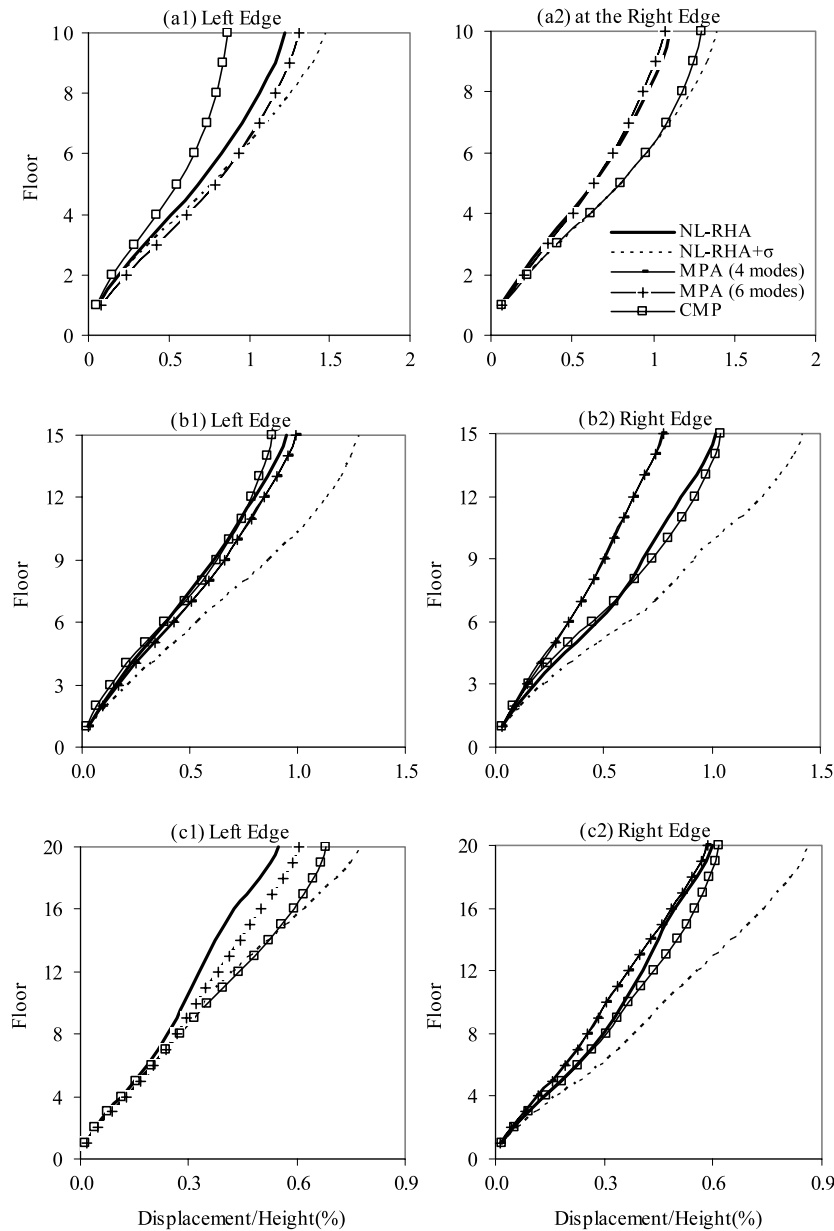
Fig. 8. Height-wise variation of the displacements at the left and right edges of torsionally-similarly-stiff systems: (a) 10-storey building; (b) 15-storey building; and (c) 20-storey building.

the symmetric-plan high-rise (20-storey) building including five modes and for all the unsymmetric-plan buildings including four and six modes. The NL-RHA was treated as a benchmark solution and conducted by using the numerical implicit *Wilson-θ* time integration method. A damping ratio of 5% was considered for the first and third modes of vibration, in order to define the Rayleigh damping matrix. Seven ground motion records were used in NL-RHA. These selected ground motions were far-field records, and corresponded to locations which were at least 12 km from a rupturing fault. More details of the ground motion records are presented in Table 2. The elastic pseudo-acceleration and displacement spectra, together with the corresponding the mean spectra, are presented, for 5% damping ratio, in Fig. 3. The records were scaled up to 0.7 and 1 g to produce nonlinear responses. The second order (*P–Δ*) effects were included within all the nonlinear static and dynamic analyses. *P–Δ* effects were also taken into consideration for all modes in the MPA and CMP procedures. The responses estimated by the aforementioned approximate pushover procedures were compared with the mean values

of maximum seismic responses obtained from seven nonlinear response history analyses (NL-RHAs). In this research, the target displacement at the roof for the CMP procedure was determined as the mean value of the maximum top floor displacements (at the CM in the *y*-direction) resulting from NL-RHAs. It is noted that this paper deals only with the effects of higher modes and torsion for the proposed procedure. Then, for the sake of examining the accuracy of this procedure in taking these effects into account, the target displacement was accurately derived from the NL-RHA. It is worthwhile noting that the target displacement can be determined by using the conventional methods. The use of these methods may result in some errors. The nonlinear version of computer program SAP2000 was used to perform nonlinear analyses [34]. It should be noted that point rigid-plastic hinges were used to represent the nonlinear behaviour in the static and dynamic analyses. Hinges were defined at the ends of the frame members. The hinge properties and relative modelling parameters were specified according to the FEMA-273 [26]. The hysteretic
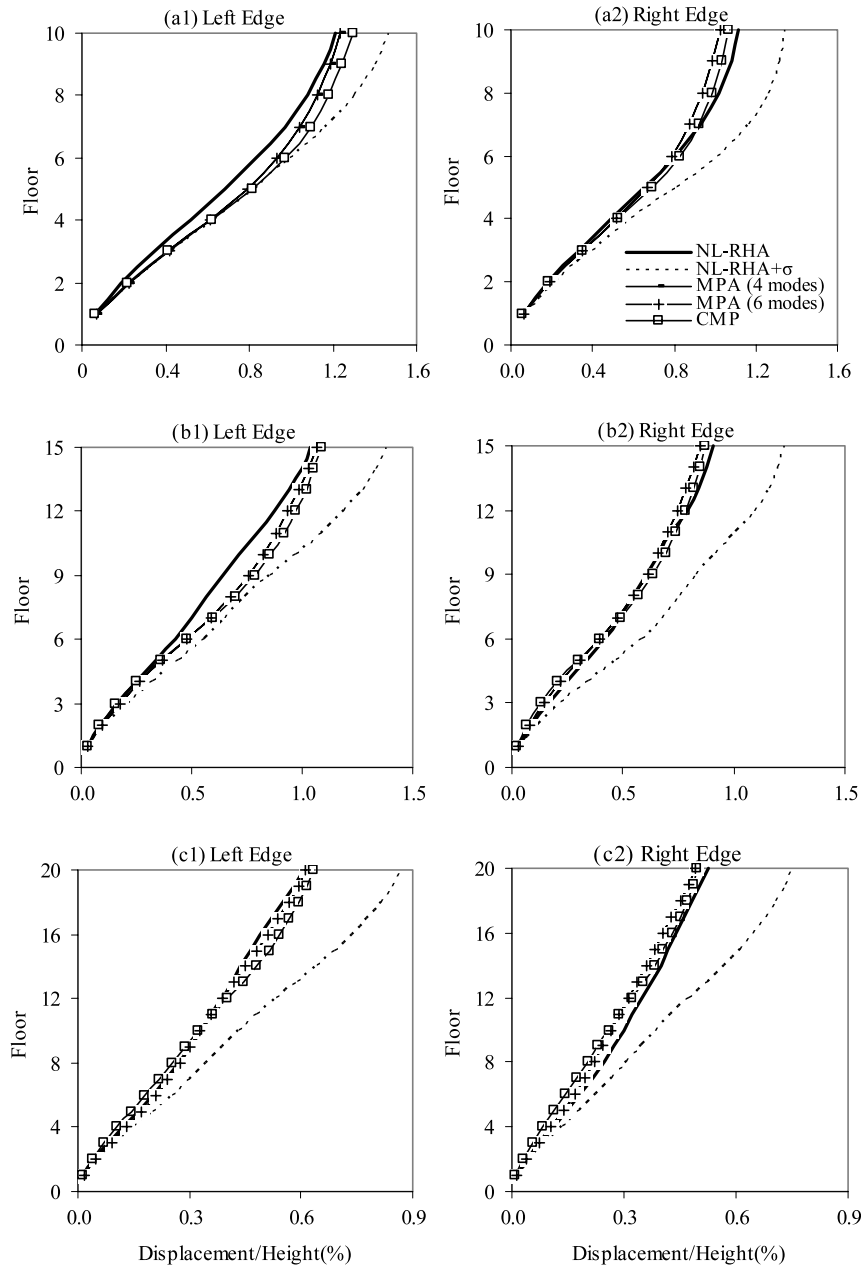
Fig. 9. Height-wise variation of the displacements at the left and right edges of torsionally-flexible systems: (a) 10-storey building; (b) 15-storey building; and (c) 20-storey building.

behaviour of the hinges is bilinear with 3% post-yield stiffness. Stiffness degradation was ignored for the NL-RHA.

7. Results and discussions

Seismic responses including floor displacements, storey drift ratios and hinge plastic rotations are presented and discussed in this chapter. Normalized top floor displacements (floor displacements from the NL-RHA at a location, in the horizontal plane, divided by displacement at the CM) are shown in Fig. 4. As seen from Fig. 4(a1) and (a2), the displacements increase at the flexible edge and decrease at the stiff edge of the torsionally-stiff systems that the trend is typical for these systems. It can be observed that normalized displacements slightly decrease at the flexible side, and increase at the stiff side of the torsionally-stiff buildings with increasing the intensity of ground motions, i.e. with increasing the

plastic deformations. This obviously implies that the effects of torsion decrease with increasing the intensity of ground motion. The results are consistent with those obtained in the previous investigations for the unsymmetric-plan low-rise buildings [20,31,35]. For the torsionally-flexible buildings, Fig. 4(c1) and (c2) show a slight decrease of displacements at the flexible edge and an increase of displacements at the stiff edge. The displacements at the stiff edge are larger than those at the centre of mass and flexible edge, indicating that the trend of torsion, in the case of the torsionally-flexible buildings, is thoroughly different from that of the torsionally-stiff buildings. As seen from figures, the increase of ground motion intensity also decreases the torsional effects for the torsionally-flexible buildings. A similar trend occurs at the other floor levels of these buildings (the results are not shown here). In the case of the torsionally-similarly-stiff buildings, the displacements not only increase at the flexible edge but also do at the stiff edge [see Fig. 4(b1) and 4(b2)]. This arises from a strong coupling
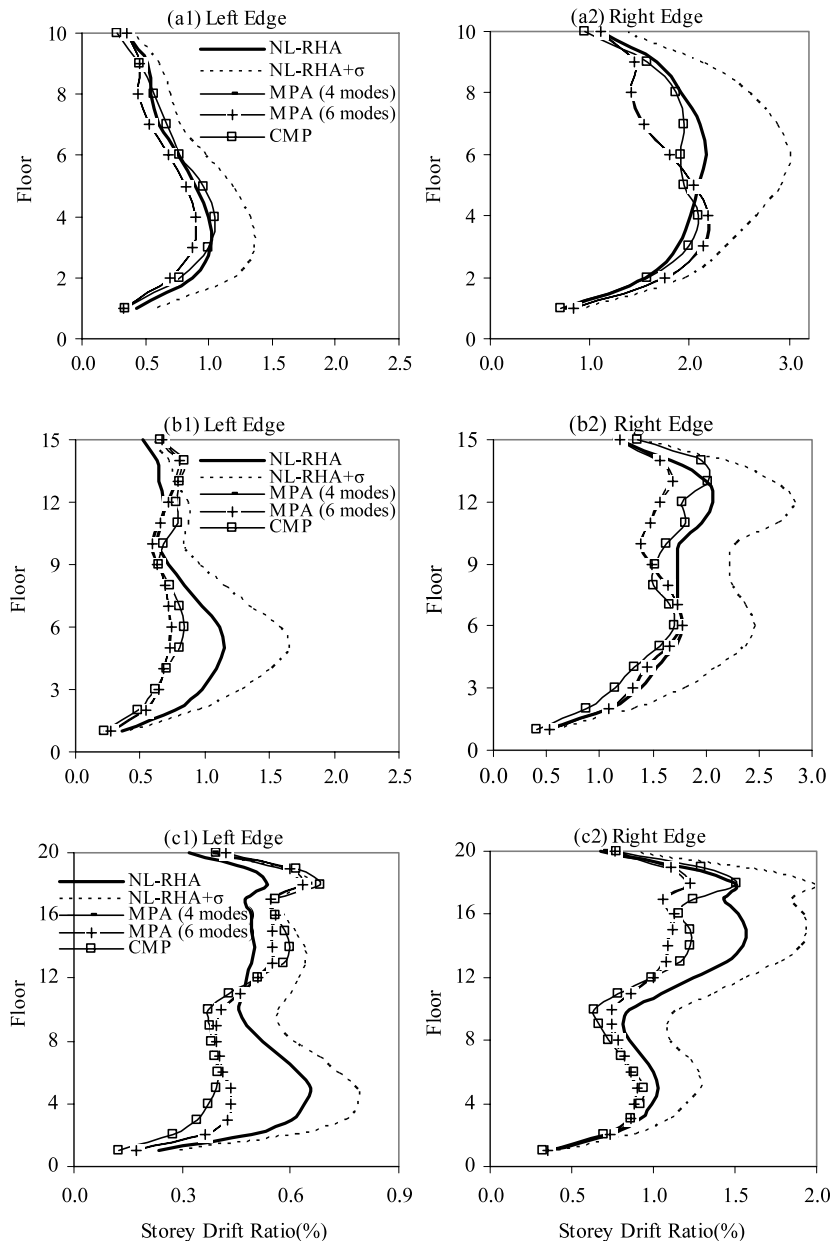
Fig. 10. Height-wise variation of the storey drifts at the left (stiff) and right (flexible) edges of torsionally-stiff systems: (a) 10-storey building; (b) 15-storey building; and (c) 20-storey building.

of the translational displacements and torsional rotations. It should be noted that the examination of the trend of torsion for different intensities of ground motions is beyond the scope of this investigation. As demonstrated above, the displacements resulting from the benchmark solution, i.e. NL-RHA are amplified at the flexible edge and de-amplified at the stiff edge of the torsionally-stiff systems. The displacements are also amplified at the stiff edge and de-amplified at the flexible edge of the torsionally-flexible systems. The figures obviously provide evidence that the CMP and MPA procedures are able to accurately consider the amplification as well as de-amplification of displacements due to the influence of torsion at the flexible and stiff sides of unsymmetric-plan buildings since these procedures use the dynamic (modal) properties of structures. As seen from Fig. 4, in the case of the torsionally-similarly-stiff systems, the line is slightly more curved than those for the other systems. Increased curvature indicates the increase in the effects of several modes of vibration [31]. Then, it can be appreciated again that more modes have to be taken into account in the extended

CMP procedure for the torsionally-similarly-stiff systems in comparison with the other systems.

Several important observations are made by considering the height-wise variation of seismic responses derived from the aforementioned analyses at the flexible and stiff edges of the unsymmetric-plan tall buildings. The results at the CM are not presented here for the briefness sake. The mean value of maximum responses from NL-RHAs and the mean value plus standard deviation (σ) have been shown. Presented in this paper for the NL-RHA (Figs. 5–15) are the results obtained by using the ground motion records which were scaled up to 1 g for all the buildings, except for the 20-storey buildings, for which they were scaled up to 0.7 g. It is noted that the CMP and MPA procedures were implemented in accordance with the relevant scaled ground motions mentioned above.

Shown in Figs. 5 and 6 are displacements and storey drifts at the CM as well as hinge plastic rotations for the interior frame's interior beam in the *y*-direction [see Fig. 1(a)] for the
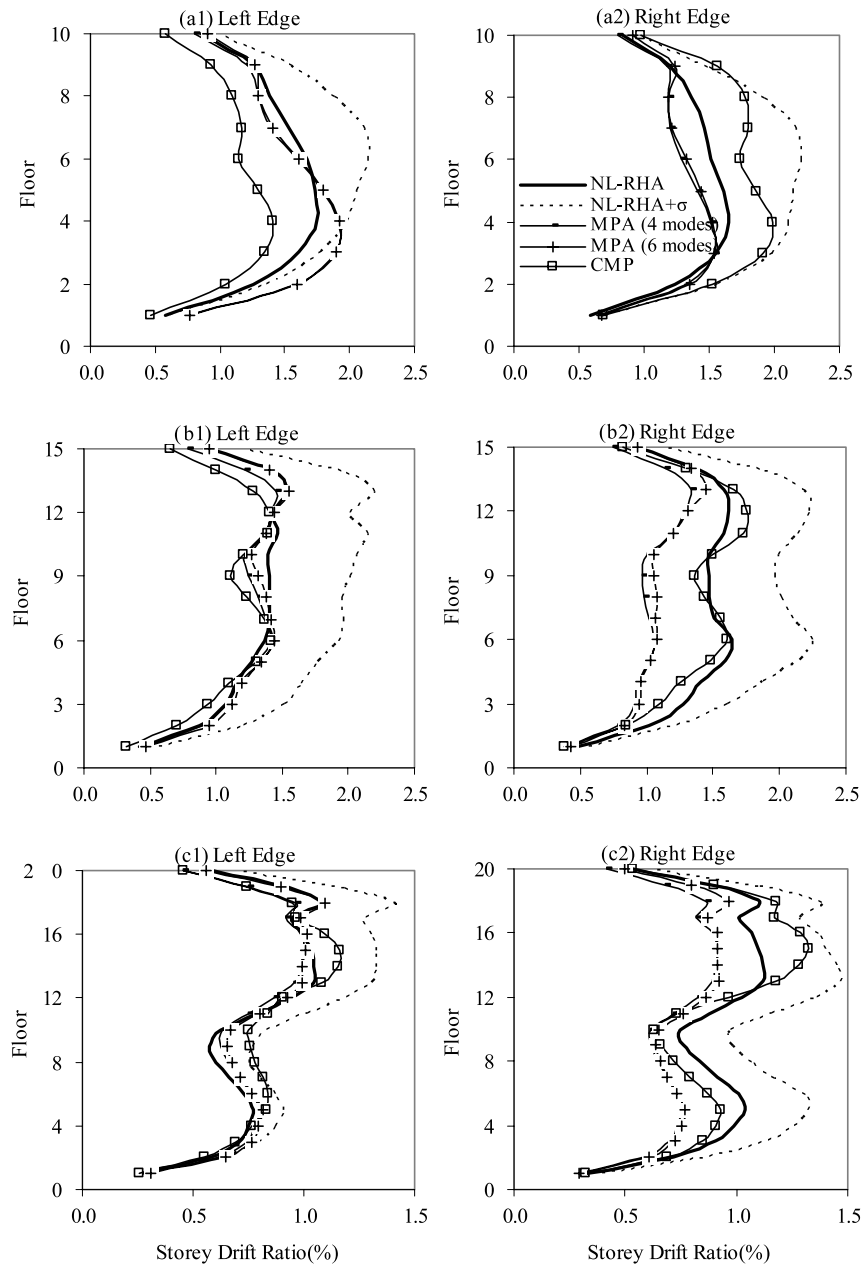
Fig. 11. Height-wise variation of the storey drifts at the left and right edges of torsionally-similarly-stiff systems: (a) 10-storey building; (b) 15-storey building; and (c) 20-storey building.

original symmetric-plan buildings. The figures illustrate that the CMP procedure, in general, provides moderately better estimates of the storey drifts than the MPA procedure for the symmetric-plan buildings. Hinge plastic rotations estimated by the CMP procedure are considerably more accurate than those obtained by the MPA procedure (see Fig. 6). Figs. 7–9 display displacements for different systems of the unsymmetric-plan buildings at the right (flexible) and left (stiff) edges. The figures demonstrate that the MPA and CMP procedures can estimate displacements with acceptable accuracy at the flexible and stiff edges of the torsionally-stiff and torsionally-flexible buildings. It is of interest to note that the displacements obtained by the MPA and CMP procedures at the flexible edge are more agreeable with the results produced by NL-RHA than those at the stiff edge. At the stiff side of the torsionally-stiff buildings, the CMP procedure provides relatively better predictions of displacements than the MPA procedure (see Fig. 7). As seen from Fig. 8, displacements

estimated by the MPA at the flexible edge and by the CMP at the stiff edge may occasionally deteriorate (be underestimated) for the torsionally-similarly-stiff buildings. Deterioration of predictions can be due to strong coupling between lateral and rotational motions in each mode of vibration [19]. Figs. 7 through 9 illustrate that the displacements, in the MPA procedure, are not influenced by including the 5th and 6th modes contributions for all the unsymmetric-plan buildings.

A comparison of storey drifts predicted by the CMP and MPA procedures with those obtained by NL-RHA indicates that estimates obtained by these approximate procedures are accurate enough for the torsionally-stiff and torsionally-flexible buildings (see Figs. 10–12). The figures illustrate that the estimates of storey drift ratios derived from the CMP procedure are more accurate (sometimes relatively more conservative) than those resulting from the MPA procedure in some cases, especially at the mid and upper storeys. In some other cases, the MPA gives better estimates
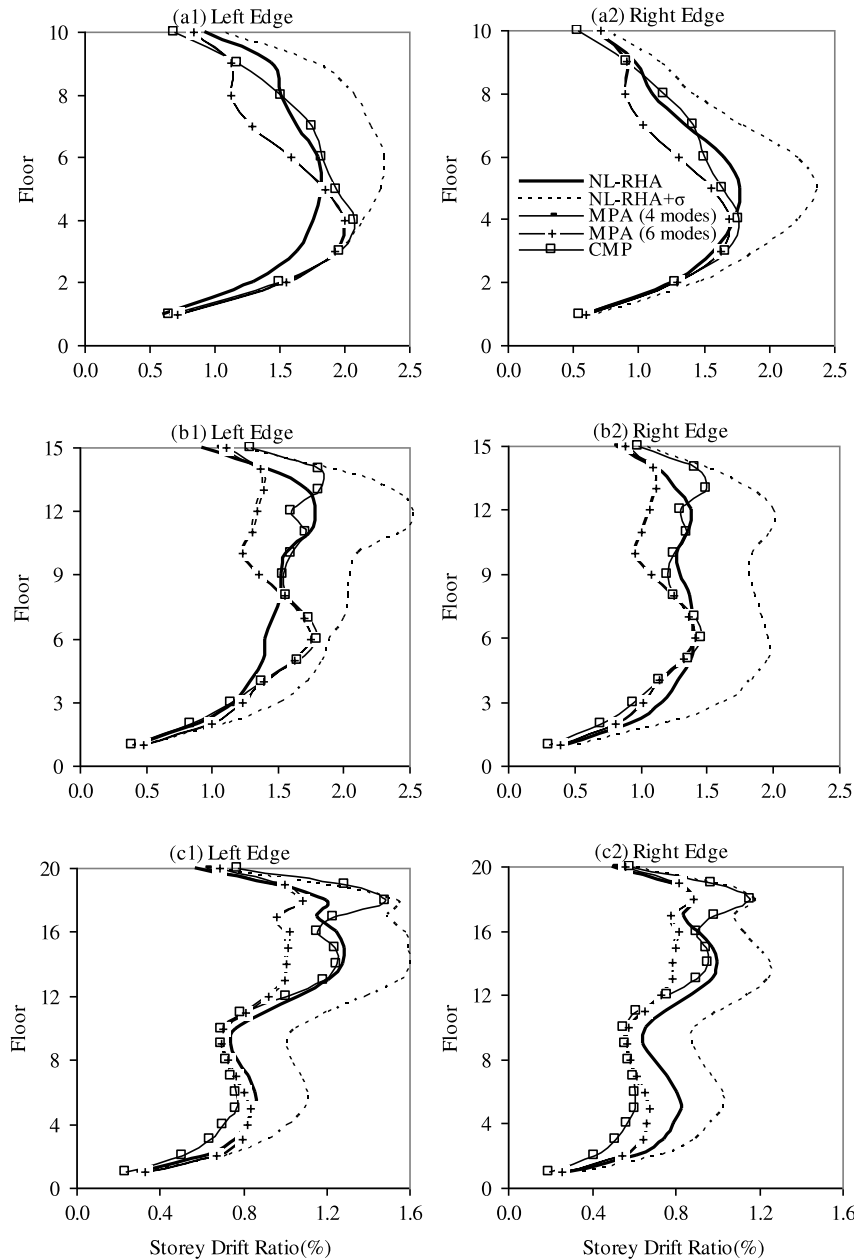
Fig. 12. Height-wise variation of the storey drifts at the left and right edges of torsionally-flexible systems: (a) 10-storey building; (b) 15-storey building; and (c) 20-storey building.

than the CMP. There is an improvement in estimating the storey drifts through the CMP at the flexible edge of the torsionally-similarly-stiff buildings (see Fig. 11), but the predictions from the CMP procedure may deteriorate to some extent at the stiff edge of these buildings in comparison with the MPA. For example, the storey drift ratios are underestimated by up to 32% by the CMP and overestimated by up to 31% by the MPA at the stiff side of the 10-storey torsionally-similarly-stiff building.

Higher modes contributions to the storey drifts are much higher than those to the displacements. As seen from Fig. 11, the storey drifts resulting from the MPA at the flexible and stiff edges of the torsionally-similarly-stiff buildings are relatively improved by including the higher (5th and 6th) modes contributions, especially at the mid and upper storeys. This improvement is negligible for the other systems of the unsymmetric-plan buildings because the modal participating mass ratios for the higher modes in the torsionally-stiff and torsionally-flexible systems are smaller than

those in the torsionally-similarly-stiff systems. Then, the higher (5th and 6th) modes contributions, in the MPA procedure, are more important in computing the storey drifts for the torsionally-similarly-stiff systems than those for the other systems.

Figs. 13–15 show the height-wise variation of hinge plastic rotations at the interior beam of the frames at the right and left sides of the unsymmetric-plan buildings. The figures clearly demonstrate that the predictions obtained by the CMP procedure are mostly in excellent agreement with results produced by NL-RHA at the flexible and stiff sides of the unsymmetric-plan buildings. The MPA procedure fails to estimate the plastic rotations with acceptable accuracy for all the unsymmetric-plan buildings and it considerably underestimates the plastic rotations. In the MPA, the plastic rotations which were computed including the contributions of six modes are the same as those obtained including the contributions of four modes since the structures remained elastic for these higher modes. The CMP
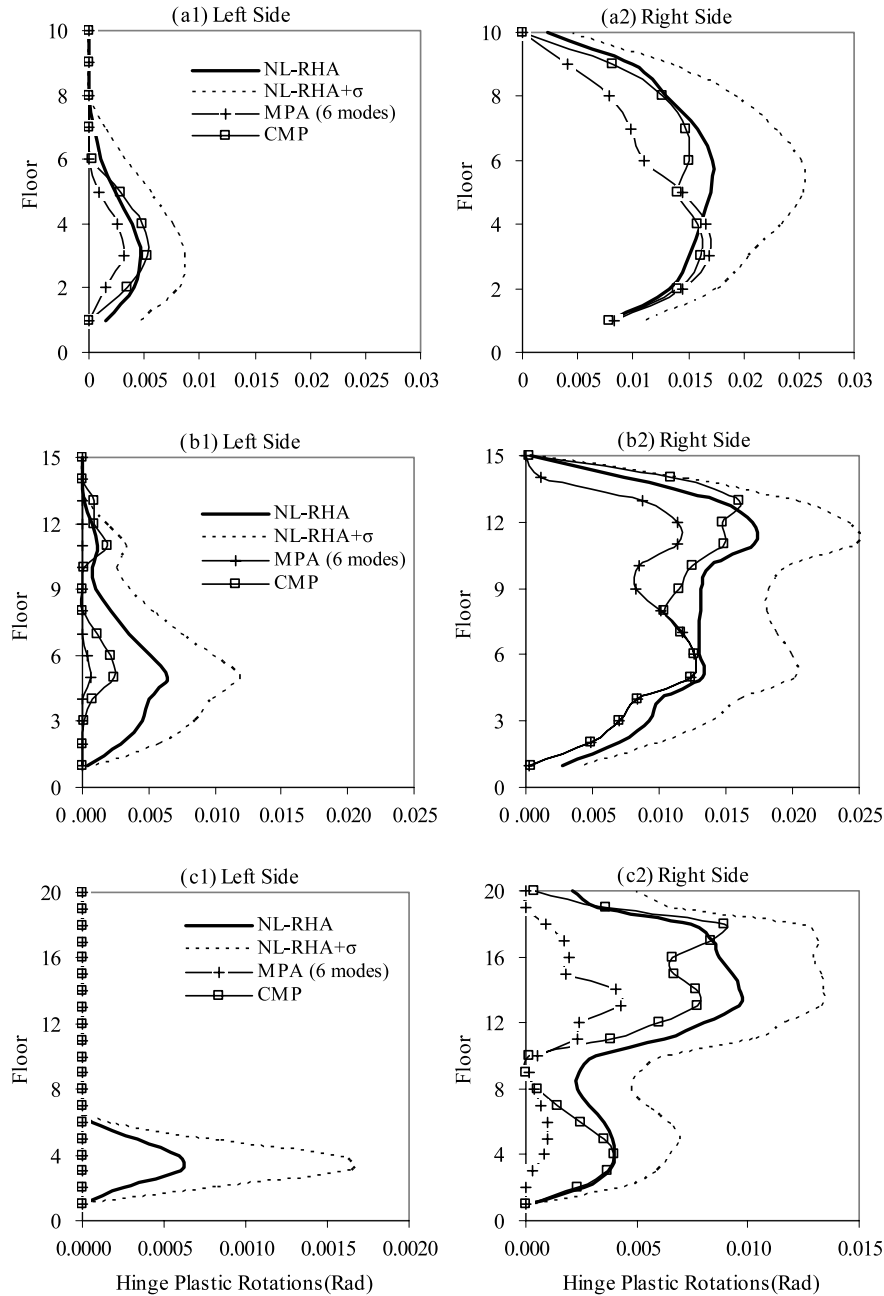
Fig. 13. Height-wise variation of the hinge plastic rotations at the left (stiff) and right (flexible) edges of torsionally-stiff systems: (a) 10-storey building; (b) 15-storey building; and (c) 20-storey building.

procedure represents a significant improvement in predicting plastic rotations at the flexible and stiff sides in comparison with the MPA procedure. The improvement is achieved by incrementally applying the lateral forces during the stages in the multi-stage pushover analysis which controls the results at the mid and upper storeys of the unsymmetric-plan tall buildings. By incrementally applying the lateral forces, rotations of the plastic hinges are consecutively accumulated. Then, the plastic hinges, in the CMP procedure, deform into the inelastic range at the mid and upper storeys, whereas in the MPA procedure they remain elastic or deform slightly into the inelastic range at these storeys because the modal pushover analyses are performed independently. It is important to note that cumulative rotations of the plastic hinges due to cyclic hysteretic behaviour are not taken into consideration

in an approximate pushover analysis such as the CMP procedure. As seen from Fig. 15, the improvement through the CMP procedure is also noticeable at the stiff side of torsionally-flexible systems where the prediction on this side was found to be so difficult in the previous investigations [21]. It is noted that the estimates of displacements and storey drifts derived from the CMP procedure are also satisfactory on the stiff side of torsionally-flexible systems (see Figs. 9 and 12).

Fig. 13(b1) and (c1) demonstrate that the hinge plastic rotations obtained by the CMP procedure are underestimated at the lower storeys on the stiff side of the 15 and 20-storey torsionally-stiff buildings. Fig. 15(c2) illustrates that the CMP procedure underestimates the plastic rotations at the lower storeys on the flexible side of the 20-storey torsionally-flexible building as well.
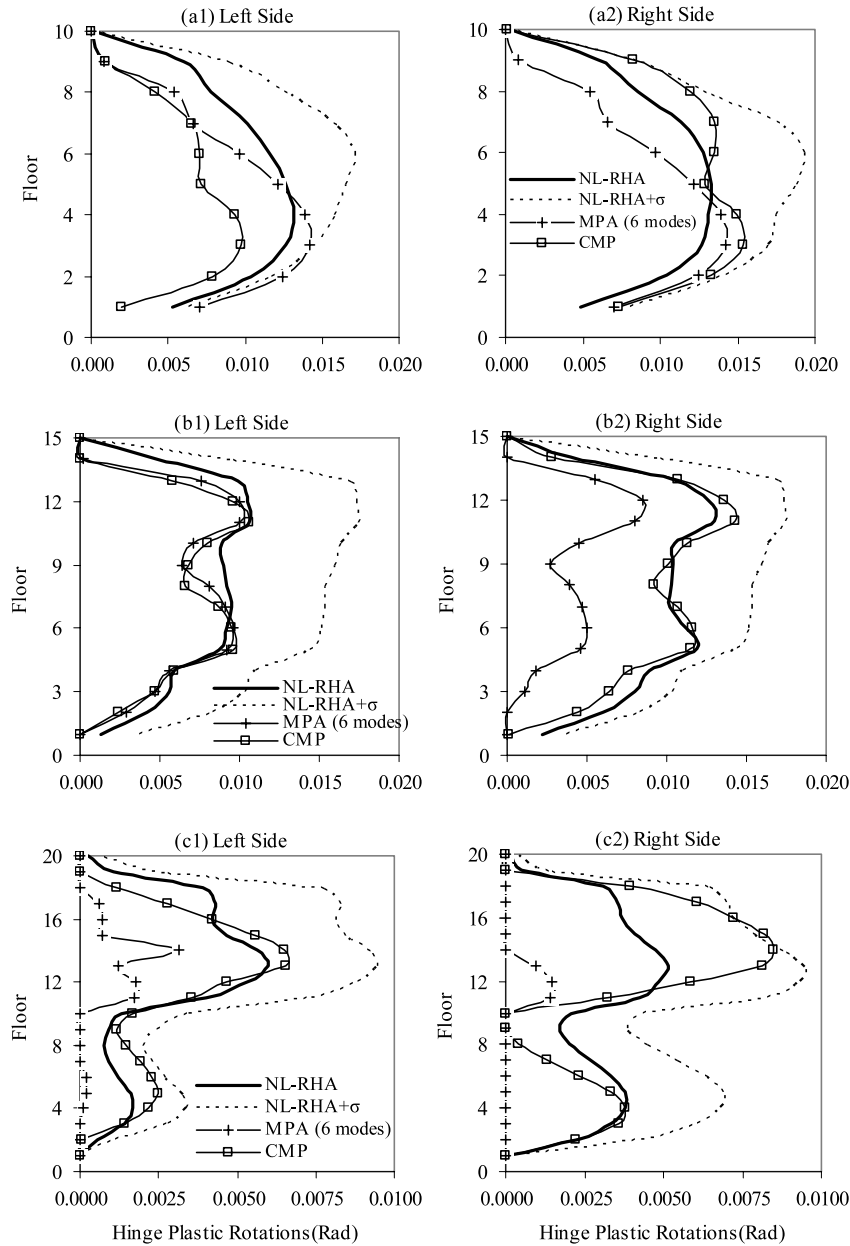
Fig. 14. Height-wise variation of the hinge plastic rotations at the left and right edges of torsionally-similarly-stiff systems: (a) 10-storey building; (b) 15-storey building; and (c) 20-storey building.

For these cases, the figures give evidence that the plastic rotations are substantially small. It was found that the dispersion of hinge plastic rotations obtained by NL-RHA for different ground motions, at the stiff side of torsionally-stiff buildings, would be generally much larger than that at the flexible side because the elements remain elastic at the stiff side of these buildings under the majority of the used ground motions. This observation is noticeable in the case of the 20-storey torsionally-stiff building. It is noted that the dispersion also depends on the intensity of ground motions. In the case of small intensity of ground motions, the elements at the stiff side of torsionally-stiff buildings may thoroughly remain elastic under the used ground motions and in the case of large intensity they may mostly deform into the inelastic range. On the other hand, in the case of moderate intensity of ground motions, the elements at the stiff edge remain elastic under several ground motions and deform slightly into the inelastic range under the rest of the ground motions. Then, the dispersion of plastic rotations, at the stiff edge of torsionally-stiff buildings, resulting from the

NL-RHA for the latter case (such as the 20-storey building in which the ground motions were scaled to 0.7 g) is significantly larger than that for the former case (such as the 10- and 15-storey buildings in which the ground motions were scaled to 1 g).

Plastic rotations obtained by the CMP procedure may be occasionally conservative at the upper storeys [see Figs. 14(c2), 15(c1) and (c2)]. In these cases, the estimates derived from the CMP procedure are in the range between the mean values of maximum rotations obtained from the NL-RHAs and the mean values plus the standard deviations. The estimates of the plastic rotations produced by the CMP may deteriorate at the stiff side of torsionally-similarly-stiff systems. It should be noted that the original symmetric-plan structures satisfied the strong column–weak beam criterion in the design process. Therefore, the yielding of the members, in general, occurred in beams.

Pushover curves resulting from the single-stage pushover analysis are shown in Fig. 16 for all the systems of unsymmetric-plan buildings. The figure provides evidence that the 10- and
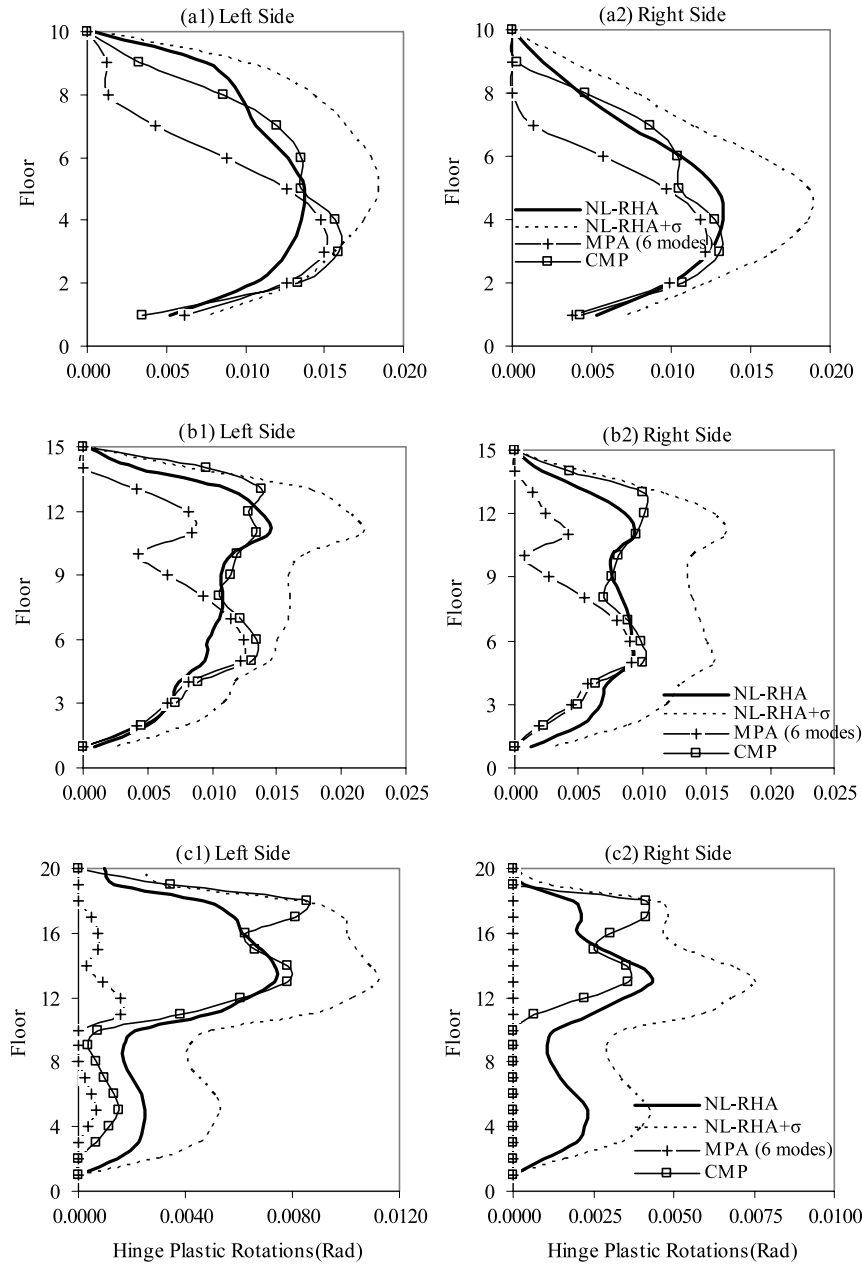
Fig. 15. Height-wise variation of the hinge plastic rotations at the left and right edges of torsionally-flexible systems: (a) 10-storey building; (b) 15-storey building; and (c) 20-storey building.

15-storey buildings deform well into the inelastic range because the records were scaled up to a larger intensity level (i.e. 1 g) for these buildings. On the other hand, different systems of the 20-storey building deform slightly into the inelastic range as shown in Fig. 16.

The behaviour of a mass-eccentric system is similar to that of a stiffness- and strength-eccentric one, in which stiffness and strength are linearly related [35]. Consequently, the CMP procedure, which was verified for mass-eccentric systems in this research, can be generalized to stiffness- and strength-eccentric systems that it would be necessary to be investigated in the other research.

8. Conclusions

This article extends the consecutive modal pushover (CMP) procedure to unsymmetric-plan tall buildings to take torsional and higher mode effects into consideration. In the CMP procedure, the

seismic responses are computed by enveloping the peak responses obtained from the multi-stage and classical single-stage pushover analyses. Linearly elastic modal properties are used in the multi-stage pushover analysis. The force distribution over the height of the building in each stage of the multi-stage pushover analysis is determined as the product of the mass matrix and relevant elastic mode-shape including both lateral and rotational components. The lateral forces are incrementally applied during the stages of the multi-stage pushover analysis. By conducting a large amount of analyses for the three types of unsymmetric-plan systems with different heights covering a wide range of periods, several important conclusions are derived.

- The CMP procedure can accurately consider the amplification or de-amplification of displacements at the flexible and stiff edges of torsionally-stiff and torsionally-flexible systems, as well as at the flexible edge of torsionally-similarly-stiff systems.
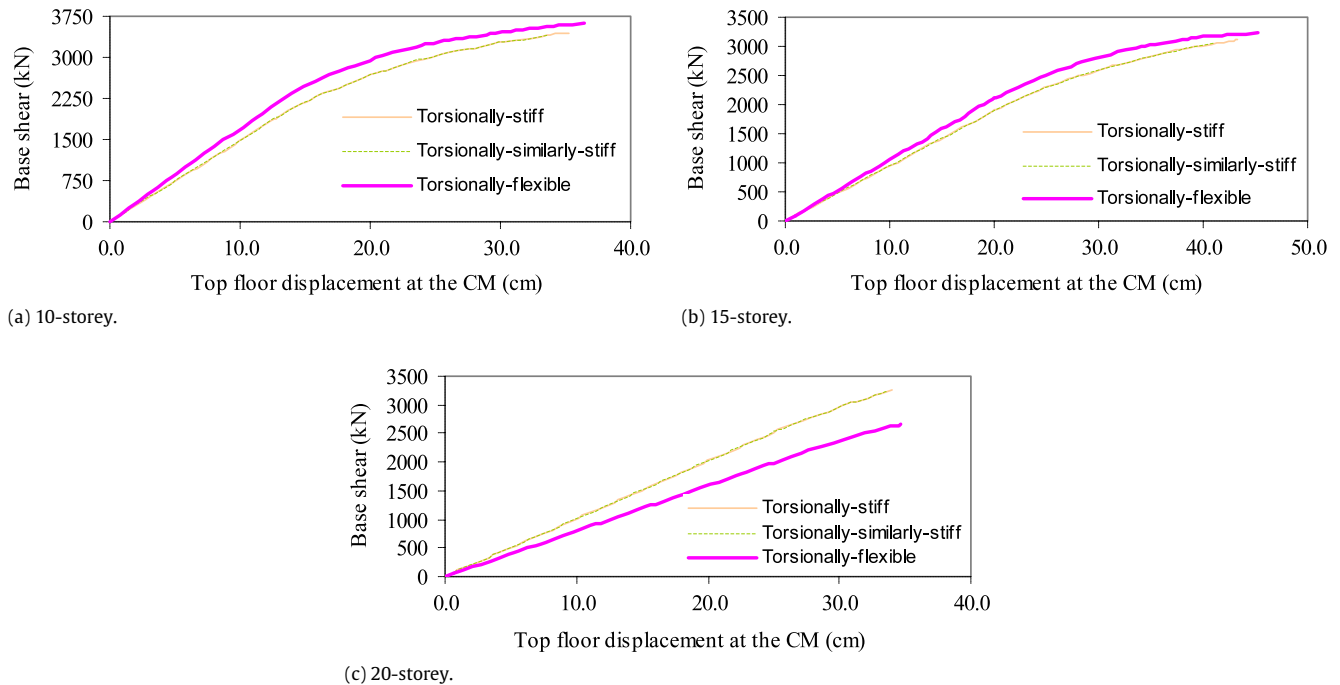
Fig. 16. Pushover curves for all the systems of unsymmetric-plan buildings with different heights: (a) 10-storey building; (b) 15-storey building; and (c) 20-storey building.

- The CMP procedure, in general, provides accurate estimates of displacements and storey drifts at both flexible and stiff edges of torsionally-stiff, torsionally-similarly-stiff and torsionally-flexible systems, except at the stiff edge of torsionally-similarly-stiff systems, for which the predictions may occasionally deteriorate to some extent due to strong coupling of the lateral and torsional motions.

- There is, in general, not a large difference between displacements and storey drifts derived from the CMP and MPA procedures. Estimates of the storey drifts from the CMP procedure may be relatively better (sometimes more conservative) than those from the MPA procedure in several cases, especially at the mid and upper storeys. In other cases, the MPA gives better estimates of storey drifts than the CMP. Displacements and storey drifts derived from the CMP are better than those derived from the MPA at the flexible edge of torsionally-similarly-stiff systems, but the MPA procedure gives better estimates than the CMP procedure at the stiff edge of these systems.

- An excellent improvement has been, in general, achieved through the CMP procedure in predicting plastic rotations of the hinges at both flexible and stiff sides of unsymmetric-plan tall buildings in comparison with the MPA procedure. The improvement is achieved by incrementally applying the lateral forces during the stages of the multi-stage pushover analysis. This results in a continuous accumulation of the plastic hinge rotations at the mid and upper storeys of unsymmetric-plan tall buildings. Plastic rotations derived from the CMP procedure may be occasionally conservative at the upper storeys. Under these circumstances, the predictions from the CMP procedure are in range between the mean values of maximum rotations derived from the NL-RHAs and the mean values plus the standard deviations.

Although the results indicate that the CMP is promising as an approximate procedure to estimate the inelastic seismic demands of unsymmetric-plan tall buildings, its effectiveness and accuracy should be verified for the other lateral-resisting systems, for more elaborate models of structures, and for a variety of ground motion suits with different intensities. Two-way unsymmetric-plan tall buildings under bi-directional ground motions should be investigated as well. The boundary value of period ($T = 2.2$ s), which was proposed for the steel moment-resisting frame buildings, needs to be examined for the other resisting systems. Also, in the case of unsymmetric-plan buildings which are taller than those studied in this investigation, the number of modes (stages) needed in the multi-stage pushover analysis, should be examined further. Research in this area continues.

Acknowledgements

Appendix. Details of members for the 10-storey building

As shown in Fig. A.1, the sections of the beams and columns are considered to be of the plate girder and box type, respectively. Specifications of the sections of the members for the 10-storey building are presented in Tables A.1–A.4. Axes A–D and 1–4 have been shown in Fig. 1(a).
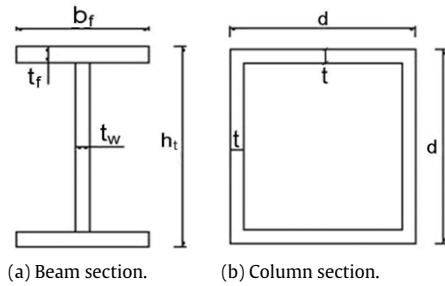
(a) Beam section.   (b) Column section.

Fig. A.1. Sections of the beams and columns.

Table A.1
Details of the sections of the columns.

Section	d (cm)	t (cm)
SC1	25	1.5
SC2	30	2
SC3	35	2.5
SC4	40	2.5
SC5	45	3

Table A.2
Details of the sections of the beams.

Section	h_t (cm)	t_w (cm)	b_f (cm)	t_f (cm)
SB1	25	0.6	17.5	1.5
SB2	30	0.8	15	1.5
SB3	30	0.8	20	1.5
SB4	35	0.8	22.5	2
SB5	40	1	22.5	2

Table A.3
Sections of the columns in the 10-storey building.

Position	Storey	Section
B1, C1, B4 and C4	1–4	SC4
	5–7	SC3
	8–10	SC2
B2, C2, B3 and C3	1–5	SC5
	6 and 7	SC4
	8	SC3
	9 and 10	SC2
A1, D1, A4 and D4	1–6	SC3
	7 and 8	SC2
	9 and 10	SC1
A2, D2, A3 and D3	1–7	SC4
	8	SC3
	9 and 10	SC2

Table A.4
Sections of the beams in the 10-storey building.

Axis	Floor	Section
1 and 4	1–7	SB3
	8–10	SB1
2 and 3	1–5	SB4
	6–8	SB3
	9 and 10	SB1
A and D	1–8	SB3
	9 and 10	SB2
B and C	1–8	SB5
	9 and 10	SB4

References

[1] Sasaki KK, Freeman SA, Paret TF. Multi-mode pushover procedure (MMP)–A method to identify the effects of higher modes in a pushover analysis. In: Proc. 6th US nat. conf. on earthq. Eng. 1998.

[2] Chopra AK, Goel RK. A modal pushover analysis procedures for estimating seismic demands for buildings. Earthq Eng Struct Dyn 2002;31:561–82.

[3] Moghadam AS. A pushover procedure for tall buildings. In: Proc. 12th European conference on earthquake engineering. London (UK): Elsevier Science Ltd.; 2002. Paper 395.

[4] Aydinoglu MN. An incremental response spectrum analysis procedure on inelastic spectral displacements for multi-mode seismic performance evaluation. Bull Earthq Eng 2003;1:3–36.

[5] Jan TS, Liu MW, Kao YC. An upper-bound pushover analysis procedure for estimating the seismic demands of high-rise buildings. Eng Struct 2004;26: 117–28.

[6] Chopra AK, Goel RK, Chintanapakdee C. Evaluation of a modified MPA procedure assuming higher modes as elastic to estimate seismic demands. Earthq Spectra 2004;20(3):757–78.

[7] Kalkan E, Kunnath SK. Adaptive modal combination procedure for nonlinear static analysis of building structures. ASCE, J Struct Eng 2006;132(11): 1721–31.

[8] Jianmeng M, Changhai Z, Lili X. An improved modal pushover analysis procedure for estimating seismic demands of structures. J Earthq Eng Eng Vib 2008;7(1):25–31.

[9] Poursha M, Khoshnoudian F, Moghadam AS. A consecutive modal pushover procedure for estimating the seismic demands of tall buildings. Eng Struct 2009;31:591–9.

[10] Kilar V, Fajfar P. Simple push-over analysis of asymmetric buildings. Earthq Eng Struct Dyn 1997;26:233–49.

[11] Kilar V, Fajfar P. On the applicability of pushover analysis to the seismic performance evaluation of asymmetric buildings. Eur Earthq Eng 2001;15: 20–31.

[12] De Stefano M, Rutenberg A. Predicting the dynamic response of asymmetric multi-storey wall-frame structures by pushover analysis: two case studies. In: Proceedings of the 11th european conference on earthquake engineering. 1998.

[13] Faella G, Kilar V. Asymmetric multi-storey R/C frame structures: push-over versus nonlinear dynamic analysis. In: Proceedings of the 11th european conference on earthquake engineering. 1998.

[14] Moghadam AS, Tso WK. Pushover analysis for asymmetrical multi-storey buildings. In: Proceedings of the 6th US national conference on earthquake engineering. Oakland (CA): EERI; 1998.

[15] Moghadam AS, Tso WK. Pushover analysis for asymmetric and set-back multi-storey buildings. In: Proc. of the 12th world conference on earthquake engineering. 2000. Paper No. 1093.

[16] Ayala AG, Tavera EA. A new approach for the evaluation of the seismic performance of asymmetric buildings. In: Proc. of the 7th national conference on earthquake engineering. 2002.

[17] Fujii K, Nakano Y, Sanada Y. Simplified nonlinear analysis procedure for asymmetric buildings. In: Proc. of the 13th world conference on earthquake engineering. 2004. Paper No. 149.

[18] Barros RC, Almeida R. Pushover analysis of asymmetric three-dimensional building frames. J Civil Eng Manag 2005;XI(1):3–12.

[19] Chopra AK, Goel RK. A modal pushover analysis procedure to estimate seismic demand for unsymmetric–plan buildings. Earthq Eng Struct Dyn 2004;33: 903–27.

[20] Fajfar P, Marusic D, Perus I. Torsional effects in the pushover-based seismic analysis of buildings. J Earthq Eng 2005;9(6):831–54.

[21] Fajfar P, Marusic D, Perus, Kereslin M. The N2 method for asymmetric buildings. In: Workshop of nonlinear static methods for design/assessment of 3D structures. 2008.

[22] Lin JL, Tsai KC. Simplified seismic analysis of asymmetric building systems. Earthq Eng Struct Dyn 2007;36:459–79.

[23] Erduran E. Assessment of current nonlinear static procedures on the estimation of torsional effects in low-rise frame buildings. Eng Struct 2008; 30:2548–58.

[24] Chopra AK. Dynamics of structures. In: Theory and applications to earthquake engineering. Third ed. Prentice Hall; 2007.

[25] Applied Technology Council, ATC-40. Seismic evaluation and retrofit of concrete buildings, Volume 1–2. Redwood City (CA); 1996.

[26] Building Seismic Safety Council (BSSC). NEHRP guidelines for the seismic rehabilitation of buildings. FEMA-273. Federal Emergency Management Agency. Washington (DC); 1997.

[27] CEN. Eurocode 8. Design of structures for earthquake resistance, part 1: general rules, seismic actions and rules for buildings. Ref. No. EN 1998-1: 2004 (E), November 2004. Brussels; 2004.

[28] Tso WK, Moghadam AS. Pushover procedure for seismic analysis of buildings. Progr Struct Eng Mater 1998;1(3):337–44.

[29] Mwafy AM, Elnashai AS. Static pushover versus dynamic analysis of R/C buildings. Eng Struct 2001;23:407–24.

[30] Fajfar P. A nonlinear analysis method for performance based seismic design. Earthq Spectra 2000;16(3):573–92.

[31] Marusic D, Fajfar P. On the inelastic seismic response of asymmetric buildings under bi-axial excitation. Earthq Eng Struct Dyn 2005;34:943–63.

[32] Standard No. 2800-05. Iranian code of practice for seismic resistant design of buildings. Third ed. Iran: Building and Housing Research Centre; 2005.

[33] AISC-ASD. Allowable stress design and plastic design specification for structural steel buildings. Chicago (IL): American Institute of Steel Construction; 1989.

[34] Computers & Structures Incorporated (CSI). SAP 2000 NL. Berkeley (CA, USA); 2004.

[35] Perus I, Fajfar P. On the inelastic torsional response of single-storey structures under bi-axial excitation. Earthq Eng Struct Dyn 2005;34(8):931–41.